Available online at www.sciencedirect.com
ScienceDirect
Vacuum 81 (2007) 663–668
VACUUM
SURFACE ENGINEERING, SURFACE INSTRUMENTATION & VACUUM TECHNOLOGY
www.elsevier.com/locate/vacuum

Electrical properties of Schottky diode Pt/SiC and Pt/porous SiC performed on highly resistif p-type 6H-SiC

K. Bourenane[a,*], A. Keffous[a], G. Nezzal[b]

[a]*Unité de Développement de la Technologie du Silicium (UDTS), 2, bd. Frantz FANON, B.P. 399, Alger-Gare Alger, Algeria*
[b]*Université Houari Boumediene (USTHB)—Institut de Génie Chimique, Algeria*

Received 17 April 2006; received in revised form 6 September 2006; accepted 19 September 2006

Abstract

We investigated the electrical characteristics of two different Schottky diode as Pt/SiC and Pt/porous SiC, elaborated on highly resistif hot-pressed p-type 6H-SiC supplied by Goodfellow. The Schottky diode was characterized in air ambient and in vacuum, this latter could be used for exhaust gas monitoring as gas sensors for different gas (O_2, H_2, CO, CO_2 and hydrocarbure). The result shows an ideality factor in range 1.1–1.5 with a barrier height varying between 0.780 and 0.950 eV function of the ambient characterization. The result indicated clearly the dependence of electrical parameters on the surface whose Schottky contact was realized (Pt) and on the ambient where the electrical tests were performed.
© 2006 Elsevier Ltd. All rights reserved.

Keywords: Silicon carbide; Schottky diode; Platinum; Porous silicon carbide

1. Introduction

It is very important to detect some harmful gases like O_2, H_2, CO, CO_2, etc. for pollution control. Boils, automobiles, etc. are major sources for these types of gases. Detection and control of these gases in high temperature has great importance. A material, which can be used in high temperature and hazardous medium, is necessary for this type of application. The recent surge of activity in wide bandgap semiconductors arose from the need for electronics devices (power MOSFET, JFET, MESFET), optoelectronics devices (Bleu LEDs), solar cells, images sensors, gas sensors and photodiodes [1–5], capable of operation at high-power levels, high temperatures and hostile environments, and separately, a need for optical materials, especially emitters, which are active in blue and ultraviolet wavelengths. Electronics based on the existing semiconductor device technologies of Si and GaAs cannot tolerate greatly elevated temperatures or chemically hostile environments due to the uncontrolled generation of intrinsic carriers and their low resistance to caustic chemicals. The wide bandgap semiconductors silicon carbide (SiC) (2.3–3.2 eV), with its excellent thermal conductivity (3–5 W/cm K) [6], large breakdown fields ($>20\times10^{-5}$ V/cm), high electron saturation velocity (2.0×10^{7} cm/s), [7] and resistance to chemical attack, will be the material of choice for these applications. In the optical device arena, the ever-increasing need for higher density optical storage and full colour display technologies are driving researchers to develop wide bandgap semiconductor emitter technologies that are capable of shorter wavelength operation. Much progress has been made in SiC for high-temperature and high-power device applications due to the availability of high-quality SiC substrates, advances in chemical vapour deposition (CVD) growth of epitaxial structures and the ability to easily dope the material both n and p types. The large Si–C bonding energy makes SiC resistant to chemical attack and radiation, and ensures its stability at high temperatures. In addition, SiC has a large avalanche breakdown field, excellent thermal conductivity and a high electron saturation velocity, all of which make it ideal for high-power operation. Metal semiconductor and metal oxide semiconductor Schottky diode with outstanding

*Corresponding author. Tel.: +213 21 43 35 11; fax: +213 21 43 24 88.
E-mail address: bourima2003@yahoo.fr (K. Bourenane).

0042-207X/$ - see front matter © 2006 Elsevier Ltd. All rights reserved.
doi:10.1016/j.vacuum.2006.09.009

high-temperature performance have already been demonstrated. In this paper, we describe the experimental process and the results of electrical parameters of two types of Schottky diode realized onto hot-pressed highly resistif p-type 6H-SiC.

2. Experimental procedure

The SiC wafers were supplied by Goodfellow (UK) as hot-pressed p-type 6H-SiC wafers with a resistivity of 30 kΩ cm. The highly resistif substrate was synonymous of the high purity. Therefore using this type of material as fabrication of gas sensors has its advantages essentially when it is allowed to use in low and high bias voltage.In fact, Barrier height change is defined as ϕ_B (air)–ϕ_B (gas). When gas (H_2 for example) concentration increases, the barrier height of the sensors decreases. It is because when more hydrogen-containing molecules come to the front electrode, more hydrogen atoms can adsorb at the electrode–substrate interface to form a polarized layer. This denser polarized layer provides a stronger electric field to further lower the barrier. The wafers were cut into slices to form squares with surface $5 \times 5\,mm^2$ and 1 mm of thickness. All samples were degreased consecutively in thrichloroethane, acetone, and methanol for a few minutes, rinsed in de-ionized water and dried with nitrogen,and then dipped into HF (10%) for a few seconds to remove the native oxide. After this procedure, a good ohmic contact was performed on the back side of the samples by using In–Ga alloy at eutectic temperature. Porous SiC layers were performed by electrochemical (anodization) method. Before this step, the samples were provided with Al contact on the front side and were annealed at 650 °C for 1 h in air; the latter allowed to reduce the electrical resistivity of SiC substrate measured by four probe. The electrochemical set-up was a standard three electrode configuration, with 6H-SiC(p) as a working electrode, a Pt sheet as a counterelectrode, and a saturated calomel electrode as reference. We used a potentiostat–galvanostat PAR 362 [8,9]. Fig. 1 shows the scanning electron microscopy image of 6H-SiC sample. The samples were then placed in a deposition chamber to evaporate a thin layer of platinum (99,998% purity). The thickness of the platinum layer was measured by RBS at 2.0 MeV at about 40.6 A (Fig. 2). This layer serves as an active area (20 mm^2) to used it later as a catalytic agent for sensors gas. Fig. 2 shows a cross-section of the SiC and Porous Silicon Carbide (PSC) schottky diode (Pt/SiC, Pt/Porous SiC–SiC).

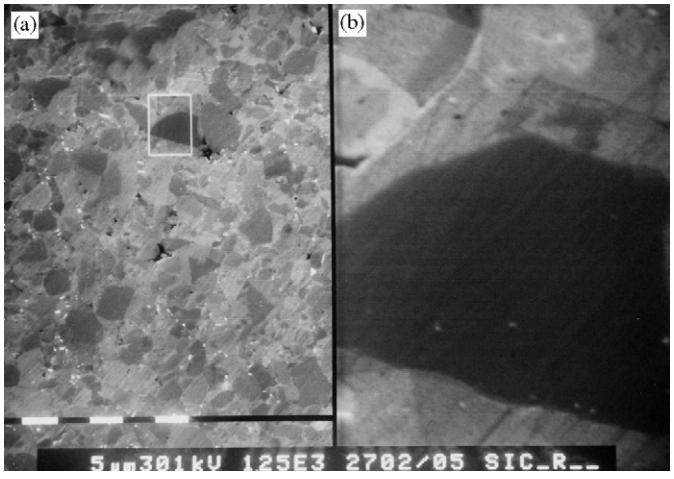

Fig. 1. Scanning electron microscopy image of bare 6H-SiC: (a) low magnification and (b) high magnification.

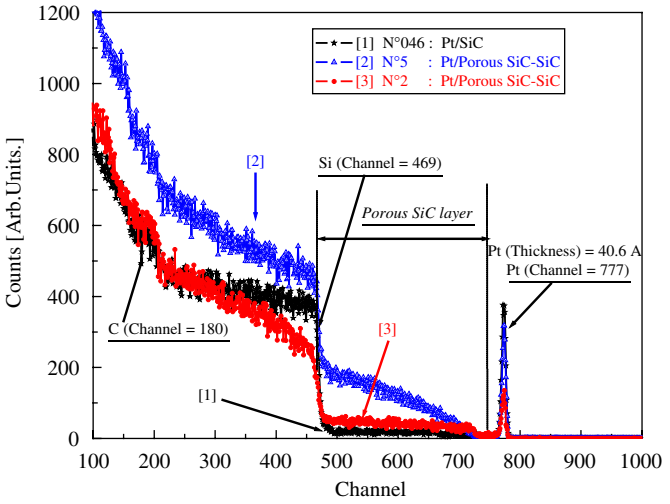

Fig. 2. RBS spectrum of Pt/SiC and Pt/porous SiC–SiC.

3. Results and discussions

3.1. Rutherford backscattering spectrometry (RBS)

The RBS spectra reveal a difference on the thickness and shape of Pt peak, this later indicates a formation of an interface layer between Pt layer and the SiC substrate, the interface corresponding to the porous SiC layer formed by the anodization of 6H-SiC in 70% HF/30% ethylene glycol (sample No. 2) and in 30% HF/70% ethylene glycol (sample No. 5) at a constant current density of 10 mA/cm^2 for 20 min etching time. Using Rump software, the thickness of Pt was found to be around 40.6 A as deposited onto bare SiC; in contrast, for the anodized SiC creation of a porous SiC layer between the substrate and Pt layer, the thickness of Pt decreases as a function of the porous SiC layer In this case the thickness is low (36 A) for samples No. 2 due to a low pore size and it was found to be 38 A less high for the sample No. 5 due to a high dissolution matter then large pore size, respectively. Fig. 3 shows the RBS spectrum of Pt deposited onto a bare 6H-SiC and onto an anodized bare 6H-SiC in different HF/ethylene glycol solution.

3.2. I–V characteristics

The forward and reverse current–voltage (*I–V*) characteristics measured on the Pt/SiC and Pt/PSC–SiC

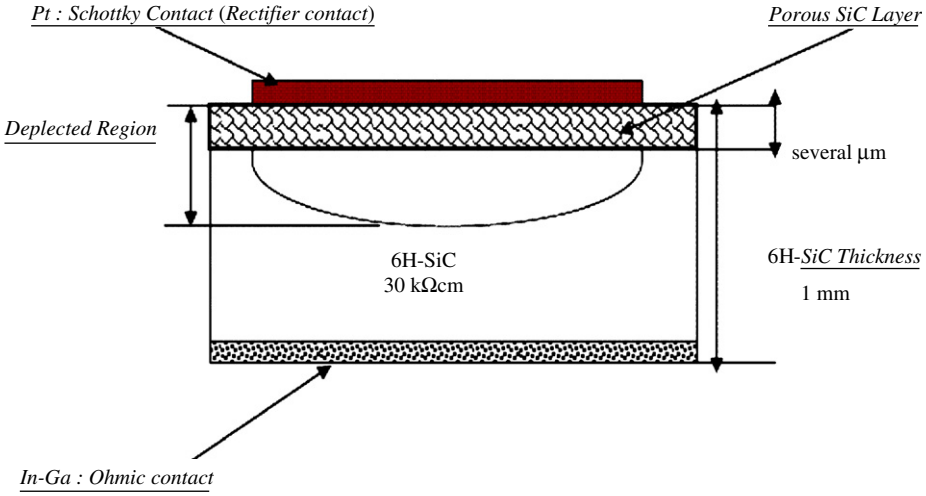

Fig. 3. Schematic cross-section view of the designed silicon carbide (SiC) Schottky diode.

Schottky diode allow for the quantitative determination of Schottky diode electrical parameters such as barrier height (ϕ_B), ideality factor (n), and series résistance (R_s) of the diodes. The I–V relationship based on the thermoionic emission–diffusion theory can be expressed as [10–13]

$$I = aA^{**}T^2 \exp\left(\frac{-q\phi_B}{kT}\right)\left[\exp\left(\frac{qV}{nkT}\right) - 1\right], \quad (1)$$

where q is the electron charge, A^{**} is the effective Richardson constant and is equal to 72 A/cm^2/K^2 for 6H-SiC [14], a is the diode area, T the absolute temperature, k is the Boltzmann constant, and ϕ_B is the barrier height.

If the barrier height ϕ_B is assumed to vary linearly with bias, one writes

$$\phi_B = \phi_{B0} + \beta V, \quad (2)$$

where ϕ_{B0} is the barrier height at zero bias and $\beta = \partial V/\partial\phi$ is the change in the effective barrier height with bias voltage. Using substitution Eq. (2), Eq. (1) becomes

$$I = I_s \exp\left(-\beta\frac{qV}{kT}\right)\left[\exp\left(\frac{qV}{nkT}\right) - 1\right], \quad (3)$$

where I_s is the saturation current,

$$I_s = aA^{**}T^2 \exp\left(\frac{-q\phi_B}{kT}\right). \quad (4)$$

By introducing a parameter n such that $1/n = 1 - \beta$, Eq. (3) can be written as

$$I = I_s \exp\left(\frac{qV}{nkT}\right)\left[1 - \exp\left(\frac{-qV}{kT}\right)\right], \quad (5)$$

where n is the ideality factor incorporating the tunnelling current in pratical diode. If the applied voltage V is much larger than kT/q, the second term in Eq. (5) becomes insignificant. The parameter n is included in the I–V relation to take into account the non-ideal behaviour. This factor is calculated from the one slop of the linear region of the forward bias Ln(I)–V:

$$n = \frac{q}{kT}\frac{dV}{d\mathrm{Ln}(I)}. \quad (6)$$

The barrier height ϕ_{B0} is determined from the extrapolated I_s and is given by the relation

$$\phi_{B0} = \frac{kT}{q}\mathrm{Ln}\left(\frac{aA^{**}T^2}{I_s}\right). \quad (7)$$

The I–V characteristics of Pt/SiC and Pt/Porous SiC–SiC Schottky diode at room temperature (295 K) were measured by a Keithley Source Measure Unit model 237 in air and are shown in Fig. 4. The ideality factor obtained from the slope of the forward I–V plot was much grater than 1 and increased when a porous SiC layer was used between Pt and SiC substrate. In contrary, when the I–V measurements were performed in vacuum (Fig. 5), we noted that Pt/SiC electrical remains constant, but for Pt/Porous–SiC–SiC we registered a decrease in all parameters, producing a high performance of electrical parameters with an ideality factor of around 1.17 and a high barrier height in order of 0.927 eV .

The forward I–V characteristics are linear in the semi-log scale but deviate from linearity due to the effect of the interface state and series resistance R_s, associated with bulk material SiC, Porous SiC–SiC, and Ohmic contact, when the applied voltage is sufficiently large [15–18]. The voltage across the diode can be expressed in terms of the total voltage drop across the diode and the resistance R_s. This is accounted for by replacing the voltage V by V–IR_s in Eq. (1). Different methods to extract the series resistance R_s have been proposed [19–21]. We applied the method developed by Cheung and Cheung [13]. Cheung's plots are determined from data of the downwards curvature region in the forward I–V plot.

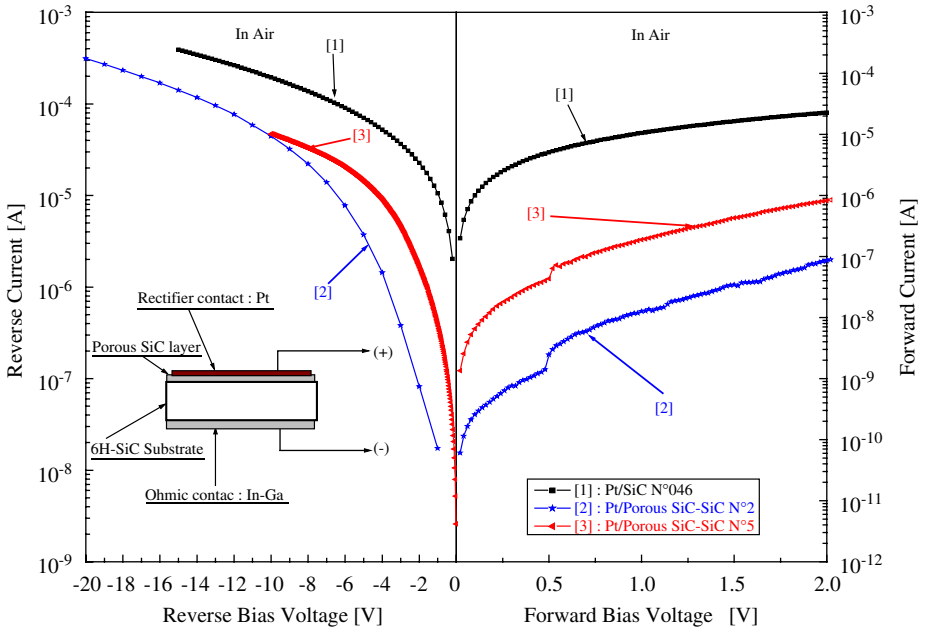

Fig. 4. Experimental forward and reverse current–voltage (I–V) characteristics of the diodes Pt/SiC and Pt/porous SiC–SiC in air.

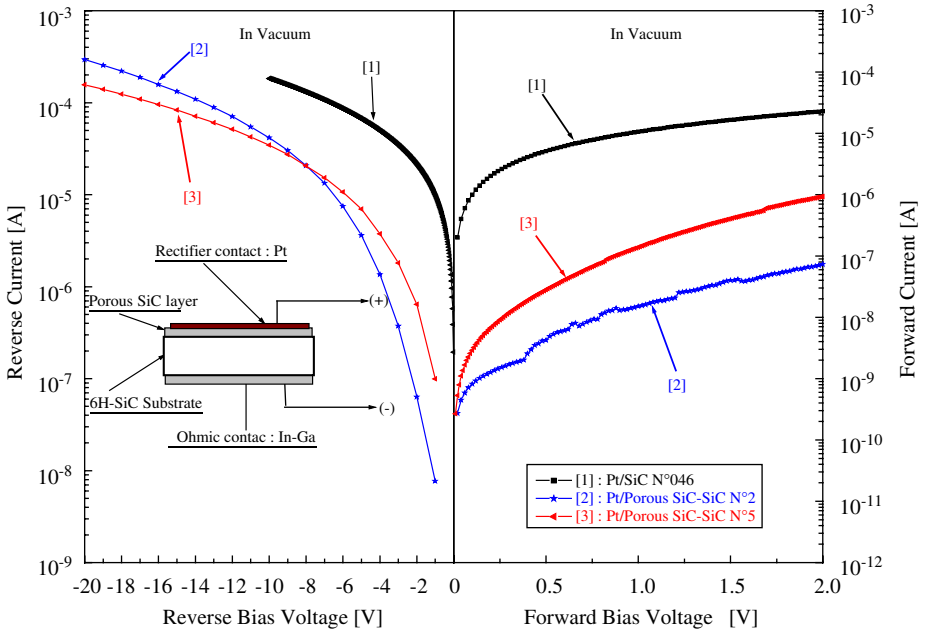

Fig. 5. Experimental forward and reverse I–V characteristics of the diodes Pt/SiC and Pt/porous SiC–SiC(p) in vacuum.

Cheung's method is achieved by using the function

$$\frac{dV}{d\,\mathrm{Ln}(I)} = IR_s + \frac{nkT}{q}. \quad (8)$$

Eq. (8) should give a straight line for the data of the downward curvature region of the forward bias I–V characteristics. The plots associated with this function are given in Figs. 6 and 7 in air and in vacuum, respectively. Thus, the slope and y-axis intercept of a plot $dV/d\,\mathrm{Ln}(I)$ vs. I will give R_s and nkT/q, respectively. The values of R_s obtained are given in Table 1.

In view of these results, one notes that when the diodes have almost ideal I–V characteristics, R_s is in the order of bulk resistivity, but when $n>1$, the series resistance takes valuethat are large multiples of resistivity. It is found that the I–V profile measured at room temperature shifts when the Schottky diode was tested in air or in vacuum.

3.3. Capacitance–voltage (C–V) characterization

In Schottky diode, the depletion layer capacitance for p-type SiC can be expressed as

$$C^{-2} = \frac{2(V + V_{bp})}{qa^2 \varepsilon_{SiC} N_A}, \quad (9)$$

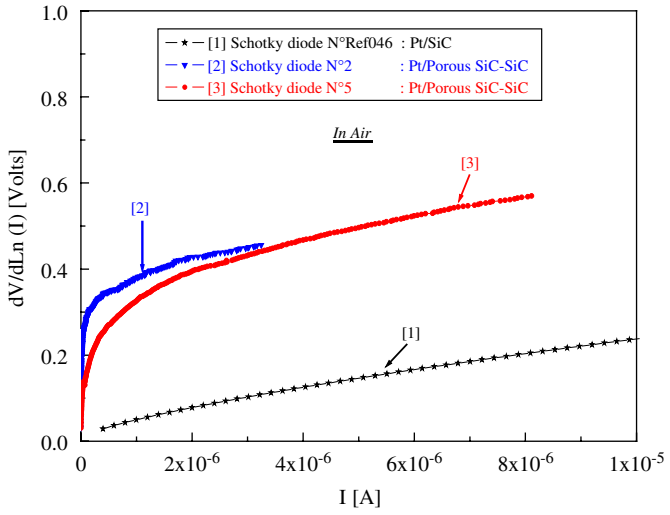

Fig. 6. Experimental $dV/d\,Ln(I)$ vs. I plots of the diodes Pt/SiC(p) and Pt/Porous SiC–SiC(p) in air.

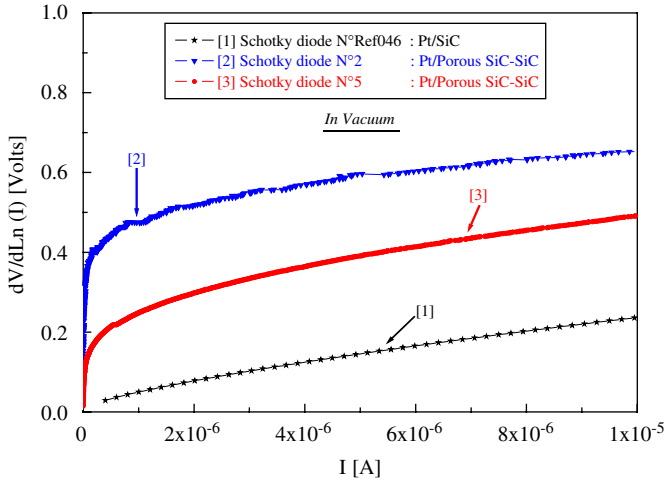

Fig. 7. Experimental $dV/d\,Ln(I)$ vs. I plots of the diodes Pt/SiC(p) and Pt/porous SiC–SiC(p) in vacuum.

where a is the area of the diode, V is the reverse voltage, V_{bp} is the flat band at zero bias and is determined from the extrapolation of C^{-2}–V plot to the V-axis, ε_{SiC} is the dielectric constant of the substrate and is equal to 9.7 for 6H-SiC, N_A is the acceptor concentration of the p-type semiconductor (substrate).

The value of the barrier height ϕ_{B0} can be obtained by the relation

$$\phi_{B0}(C - V) = V_{bp} + V_p, \quad (10)$$

where V_p is the potential difference between the Fermi level and the bottom of the valence band (E_F–E_V) in the natural region of p-type SiC and can be calculated knowing the carrier concentration as

$$V_p = \frac{kT}{q} \mathrm{Ln}\left(\frac{N_V}{N_A}\right), \quad (11)$$

where T is the temperature measurement (room temperature 295 K), k is the Boltzmann constant ($k = 1.38 \times 10^{-23}$ J/K); and N_V is the effective density of the valence, at room temperature $N_V = 2.513 \times \cdot 10^{19}$ cm^{-3}.

The C–V characteristics were measured in air and in vacuum at room temperature (295 K), by an Agilent 4278A capacitance meter at 1 MHz the variation of the barrier height caused by changing the ambiant was evaluated from

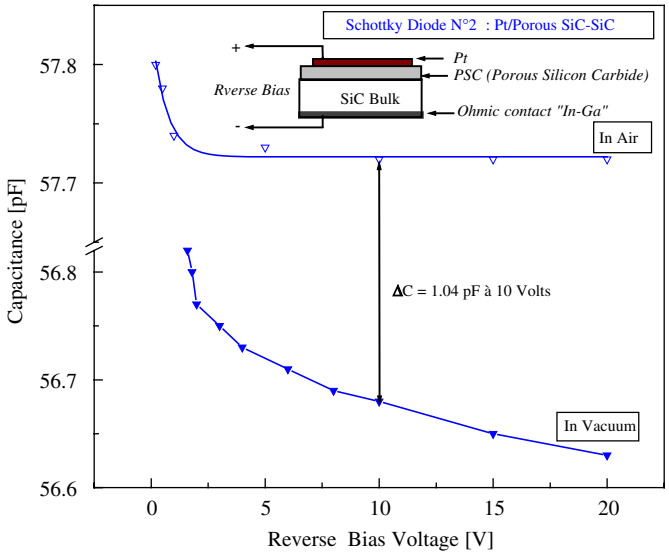

Fig. 8. C–V characteristics in air and in vacuum of the diode Pt/porous SiC–SiC(p) prepared in 30% HF/70% ethylene glycol for 20 min.

Table 1
Electrical parameters by IV measurements of different silicon carbide and porous silicon carbide Schottky diode

	In air					In vacuum				
	n	I_s (nA)	V_{bp} (V)	ϕ_{Bp} (eV)	R_s (kΩ)	n	I_s (nA)	V_{bp} (V)	ϕ_{Bp} (eV)	R_s (kΩ)
Diode No. 046 Pt/SiC	1.137	500	0.671	0.726	8.23	1.137	500	0.671	0.726	6.81
Diode No. 2 Pt/PSC/SiC	1.244	0.3	0.971	0.915	31.21	1.606	1.0	0.797	0.884	7.29
Diode No. 5 Pt/PSC/SiC	1.220	5.0	0.790	0.843	27.99	1.172	1.5	0.927	0.874	9.32

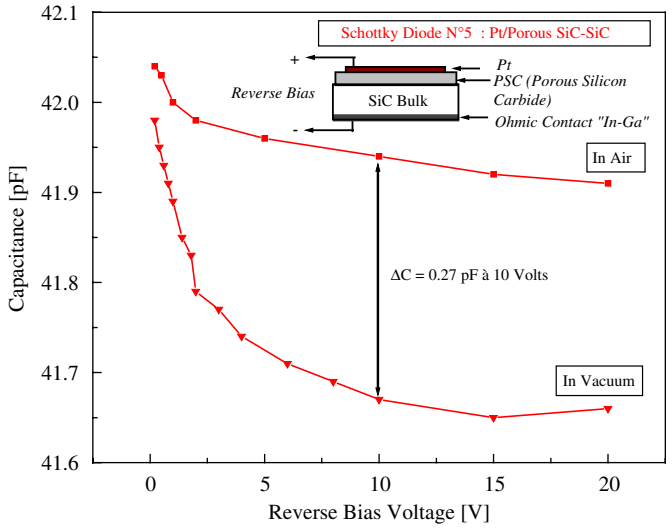

Fig. 9. *C–V* characteristics in air and in vacuum of the diode Pt/porous SiC–SiC(p) prepared in 70% HF/30% ethylene glycol for 20 min.

C^{-2} vs. *V*. Figs. 8 and 9 show *C–V* characteristics of Pt/Porous SiC–SiC in air and in vacuum for two Schottky diodes with different morphology of Porous SiC realized by a solution 30% HF/70% ethylene glycol and 70% HF/30% Ethylene glycol for 20 min anodization time, respectively.

4. Conclusion

In conclusion, to improve the performances of the SiC Schottky diode electrical parameters, a better initial determination of electrical parameters of the two type Schottky structure: Pt/SiC and Pt/Porous SiC–SiC has been found and has attracted much early interest because of its fabrication simplicity. The use of Platinum as Schottky contact on high resistif hot-pressed SiC with low thickness allows to obtain satisfactory results, such as an ideal factor around 1.172 with a barrier height ϕ_{Bp} with a value of 0.927 eV. The following work in the first times, is the study of the electrical behaviour of these Schottky diodes in different gas ambients such as: CO, O_2, H_2 and CO_2, then, in the second is the realization of Schottky diode with thin layer SiC deposited onto silicon by the PLD using laser KrF excimer.

References

[1] Myons SY, Kim SS, Lin KS. Appl Phys Lett 2004;84:5416.
[2] Ma TF, Xu J, Du JF, Li W. J Appl Phys 2000;88:6408.
[3] Chang SS, Saka A. Mater Lett 2004;58:1212.
[4] Fernades M, Vieira M, Rodrignes I. Sensors Actuators 2004; A113:360.
[5] Akiyama M, Hamada M, Takao H, Sawada K, Ishida M. Jpn J Appl Phys 2002;41:2552.
[6] Ferrero S. Ph.D. thesis, Dptm. Elettronica Politecnico di Torino, February 2002.
[7] de Lagemaat JVan, Makelbergh DVan, Kelly JJ. J Appl Phys 1998;83:6089.
[8] Shor S, Grimberg I, Weiss BZ, Kurtz AD. Appl Phys Lett 1993; 62:2836.
[9] Matsumoto T, Takahashi J, Tamaki T, Futagi T, Minura H, Kanemitsu Y. Appl Phys Lett 1994;64:226.
[10] Sze SM. Physics of semiconductor devices. 2nd ed. New York: Wiley; 1981.
[11] Rhoderick EH, Williams RH. Metal–semiconductor contacts. 2nd ed. Oxford University Press: Oxford; 1988.
[12] Rahab H, Keffous A, Siad M, Boussaa N, Menari H. Nucl Instrum Methods A 2001;453:413.
[13] Cheung SK, Cheung NW. Appl Phys Lett 1986;49:85.
[14] Waldrop JR, Grant RW, Wang YC, Davis RF. J Appl Phys 1992; 72:4757.
[15] Harris CI, Savage S, Konstantinov A, Bakowski M, Ericsson P. Appl Surf Sci 2001;184:393.
[16] Matsumoto T, Takahashi J, Tamaki T, Futugi T, Mimura H, Kanemitsu Y. Appl Phys Lett 1994;64:226.
[17] Liao LS, Bao X, Yang ZF, Min NB. Appl Phys Lett 1995;66:2382.
[18] Turut A. Phys B 1995;205:41.
[19] Lien CD, So FCT, Nicolet MA. IEEE Trans Electron Dev 1984; ED–31:1502.
[20] Bohlin KE. J Appl Phys 1986;60:1223.
[21] Manifacier, et al. J Appl Phys 1988;6:2502.